NATIONAL AERONAUTICS AND SPACE ADMINISTRATION

46p

PROPOSED JOURNAL ARTICLE

(NASA TMX-51459)

THE EFFECT OF PERIPHERAL WALL CONDUCTION ON LAMINAR FORCED CONVECTION IN RECTANGULAR CHANNELS

By Robert Siegel and Joseph M. Savino

NASA, Lewis Research Center,
Cleveland, Ohio

5 Dec. 1963 rejd

Submitted for Publication

Prepared for

Journal of Heat Transfer

December 5, 1963

THE EFFECT OF PERIPHERAL WALL CONDUCTION ON LAMINAR FORCED CONVECTION IN RECTANGULAR CHANNELS

by Robert Siegel and Joseph M. Savino

Lewis Research Center
National Aeronautics and Space Administration
Cleveland, Ohio

E-2330

ABSTRACT

This study deals with fully developed laminar forced convection in rectangular channels that are heated on the broad sides. The analysis determines the effect of peripheral heat conduction within the heated walls on the wall temperature distributions. The unheated short side walls are assumed nonconducting. The heat conduction within the broad walls was formulated in terms of an integral equation and coupled with the convective energy equation within the fluid. Solutions are given where the heating extends over the entire width of the broad side, is removed from the corner region, or extends beyond the corner into the side wall. Transverse wall conduction produced substantial decreases in the peak wall temperature and in the temperature gradients along the long side. For channels having the same heat generation per unit length, an aspect ratio of 20 or larger yielded the minimum peak temperatures for any value of the thermal conductivity.

NOMENCLATURE

A_n Fourier coefficients defined by eq. (10)

$\bar{A}_n$ coefficients defined by eq. (11b)

a	half-length of the short side of a rectangular duct
b	half-length of the long side of a rectangular duct
C_n	integral coefficients given by eqs. (14) and (17)
c_p	specific heat of fluid at constant pressure
c	half-length of heated region on broad sides
E_n	Fourier coefficients given by eqs. (16) and (20)
e	distance heated region extends into side plate
G	quantity defined in eq. (A2)
K	wall-to-fluid conduction parameter, wk_w/ak_f
k	thermal conductivity
p	static pressure
Q	total heat-transfer rate to fluid per unit channel length
q_g	heat generation rate in wall per unit area
R_n, S_n	Fourier coefficients defined by eqs. (A5) and (A7)
T	temperature
u	local fluid velocity
$\bar{u}$	integrated mean fluid velocity
w	thickness of channel wall
X	dimensionless coordinate, x/a
x	coordinate measured from center of duct in a direction parallel to short side
Y	dimensionless coordinate, y/b

y coordinate measured from center of duct in a direction parallel to long side

z coordinate measured along duct length

γ aspect ratio of rectangular duct, b/a

θ dimensionless temperature, $4k_fT/Q$

μ absolute fluid viscosity

ν coordinate pertaining to normal derivative

ρ fluid density

Subscripts:

b integrated mean value

f fluid

L Laplace solution

P Poisson solution

w wall

INTRODUCTION

It is common in many nuclear reactors to utilize fuel assemblies in which a series of parallel fuel bearing plates are closely spaced and supported along their edges by unfueled side plates (fig. 1(a)). This array forms a set of rectangular channels through which the coolant flows. Most of the heat is generated in the fueled portion of the broad plates with a small amount being produced by gamma heating in the unfueled portion and side plates. A typical fuel plate is composed of a thin layer of uranium fuel pressed between two thin metal

plates. Current practice is to have the edge of the fuel loading terminate a specified distance away from the side plate (fig. 1(a)). The reason for retaining a short unfueled width adjacent to the corner is to avoid transferring heat directly into what is believed to be a region of poor convection resulting from low velocities or the presence of a laminar region when the core of the fluid is turbulent.

Before a reactor is operated at its design power level it is necessary to know with some degree of accuracy the wall temperature distributions in any cooling channel. In particular, it is important to know the magnitude and location of the maximum wall temperature since excessively high values can lead to fuel assembly failures and serious reactor damage.

The wall temperature distribution in a cooling channel is influenced by many factors such as the coolant velocity, distribution of heat generation along the walls, channel aspect ratio, thermal conductivity of the wall material, and width of the unfueled region in the fuel plates. Many of these factors are interrelated in a complicated manner, and, to determine the combined effect of certain ones, it is necessary to analyze simplified models that retain the essential features of the general problem.

Some studies of forced convection in rectangular channels have been reported in the literature. Cheng [1] obtained an analytical solution for laminar flow in a channel that was uniformly heated on all four sides, and evaluated the wall temperatures for aspect ratios of 1, 2, and 4. Sparrow and Siegel [2] used variational methods to analyze channels with

uniform heating on all four sides, and also obtained a solution with uniform heating on only the two broad walls for an aspect ratio of 10. Savino and Siegel [3] provided the analytical solution for the case in which the sides of the channel are uniformly heated, but the heat flux on the short sides is an arbitrary fraction between 0 and 1 of the flux on the broad sides. Their analysis showed that the peak wall temperatures were lowest when all the heat was transferred through the broad walls only, and the aspect ratio was increased to about 10 or 20. Beyond 20 there was no additional temperature decrease of significance. In ref. 4, a situation was analyzed wherein the heating, which could be uniform or nonuniform, occurred only on the broad walls but was removed various short distances from the side wall. As the width of the unfueled region was increased, the peak temperature shifted from the corner to the center of the broad wall.

For all the cases mentioned, the walls were assumed to be nonconducting so that the heat was convected away at the local position where it was generated. In an actual channel, the wall would be conducting so that some of the heat generation would flow peripherally within the wall and tend to equalize the wall temperature distribution. Eckert and Low [5] analyzed numerically the fully developed turbulent heat transfer in isosceles-triangular and rectangular (aspect ratio, 5) passages to determine the effect of peripheral conduction in the walls when the walls were heated internally. The results showed how the wall temperatures

decreased and became more uniform as the ratio of the wall to fluid thermal conduction was increased, but the additional effect of aspect ratio was not treated. Baumeister and Reilly [6] studied, by a finite difference method, the heat transfer in the corner region of a rectangular cooling channel for a specific set of conditions. A single value of the heat-transfer coefficient on each wall was assumed. Although conduction in the wall was included, the results were too limited to provide general conclusions on the effect of wall conduction.

In the present paper the combined effects of peripheral wall conduction, aspect ratio, and width of the unheated region in the corner will be examined. To simplify the analysis, it is assumed that only the broad heat-generating sides are conducting and that the short side walls are of insulating material with zero conductivity. Dimensionless wall temperature distributions are evaluated for several aspect ratios and spacings of the fuel loading away from the corner. Some cases are also given where the fueled region extends beyond the corner and into the side plates. The dependence of the maximum wall temperature on the aspect ratio is shown for all values of the wall conductivity.

ANALYSIS

For this study, the typical fuel assembly cooling passage shown in fig. 1(a) has been approximated by the model in fig. 1(b). A half-thickness of the fuel plate has been replaced by a homogeneous conducting plate with internal heat generation over a width along the broad

side equal to that of the fuel loading. The small amount of gamma heating generated in the unfueled regions of the walls is neglected. However, because the entire broad wall has a nonzero thermal conductivity, heat is conducted into its unfueled region and then transferred to the fluid in the corner. The broad walls are assumed to be sufficiently thin so that the temperature is constant through the wall thickness and equal to the local fluid temperature at the wall. The short side walls are assumed to be of insulating material having zero thermal conductivity, which idealizes somewhat the practical situation where there is a poor thermal bond at the joint between the fuel plate edge and the side plate. The assumptions are made that the flow is laminar and that the fluid has constant properties. The region under study is restricted to axial locations sufficiently far from the channel entrance so that the velocity and temperature profiles are fully developed. In order that the temperatures can be compared on an equivalent basis, the total heat generated per unit channel length is kept the same for all aspect ratios and configurations of the heat-generation distribution in the walls.

Since the convective term in the energy equation involves the velocity distribution, the first step in the analysis is to specify the velocity variation over the cross section. With the assumption of constant fluid properties, the velocity distribution can be obtained independent of the energy equation since the viscosity is not influenced by the temperature distribution.

Velocity distribution. - For fully developed steady laminar flow, the momentum equation in rectangular coordinates is given by

$$\frac{dp}{dz} = \mu \left(\frac{\partial^2 u}{\partial x^2} + \frac{\partial^2 u}{\partial y^2} \right) \tag{1}$$

The solution for $u(x,y)$ is available in Knudsen and Katz [7], page 101 as well as in a number of other references, including some dealing with the stress function for torsion of a rectangular bar. The expression used here has been placed in a form especially suitable for evaluation by a computer:

$$\frac{u}{\bar{u}} = \frac{1 - X^2 + \frac{32}{\pi^3} \sum_{n=1,3,5,\ldots}^{\infty} \frac{(-1)^{\frac{n+1}{2}}}{n^3} \left[\frac{e^{-\frac{n\pi\gamma}{2}(1-Y)} + e^{-\frac{n\pi\gamma}{2}(1+Y)}}{1 + e^{-n\pi\gamma}} \right] \cos \frac{n\pi X}{2}}{\frac{2}{3} - \frac{128}{\gamma\pi^5} \sum_{n=1,3,5,\ldots}^{\infty} \frac{1}{n^5} \left(\frac{1 - e^{-n\pi\gamma}}{1 + e^{-n\pi\gamma}} \right)} \tag{2}$$

Energy equation. - The energy equation in the fluid expresses a balance between the energy conducted into and convected away from a differential volume:

$$\rho c_p u \frac{\partial T}{\partial z} = k_f \left(\frac{\partial^2 T}{\partial x^2} + \frac{\partial^2 T}{\partial y^2} + \frac{\partial^2 T}{\partial z^2} \right) \tag{3}$$

Viscous dissipation has been assumed negligible. For steady conditions the wall heating per unit channel length Q must be carried away by

convection. This leads to the overall energy balance

$$4ab\rho c_p \bar{u} \frac{\partial T_b}{\partial z} = Q$$

For fully developed conditions, the temperature profile retains the same shape for all z so $\partial T/\partial z = \partial T_b/\partial z$, and, therefore,

$$\frac{\partial T}{\partial z} = \frac{Q}{4ab\rho c_p \bar{u}}; \qquad \frac{\partial^2 T}{\partial z^2} = 0$$

Substituting into eq. (3) gives

$$\frac{Q}{4ab}\frac{u}{\bar{u}} = k_f\left(\frac{\partial^2 T}{\partial x^2} + \frac{\partial^2 T}{\partial y^2}\right) \text{ or } \quad \nabla^2\theta = \frac{1}{ab}\frac{u}{\bar{u}} \tag{4}$$

where the temperatures T have been nondimensionalized by $Q/4k_f$ to produce θ. This Poisson equation, with $u/\bar{u}$ given by eq. (2), is to be solved subject to boundary conditions that account for peripheral heat conduction in the broad duct wall.

Cases I(a) and (b). - Heating extends part way and all the way to the corner, respectively. - With reference to fig. 1(b), all the cases considered herein will have equal heat generation per unit volume on both broad sides, and the fuel will be distributed symmetrically about the x-axis. Hence, from symmetry, only one quarter of the channel cross section need be considered, and the upper right quadrant is selected as shown in fig. 2. For case I, the heating extends from $y = 0$ to $y = c$ where $c \leq b$; thus, the energy source can extend all the way to the corner or be removed a distance d away from the corner.

As discussed in ref. 8, if, for a given geometry, a solution of Poisson's equation is known for simple boundary conditions, then more involved boundary conditions can be accounted for by superimposing solutions of Laplace's equation. An analytical solution of Poisson's equation is available in ref. 3 for the case where uniform heating extends on the broad wall from $y = 0$ to b, there is no heating in the side wall, and both walls are all nonconducting. This solution is called θ_P and satisfies the equation

$$\nabla^2\theta_P = \frac{1}{ab}\frac{u}{\overline{u}} \tag{5}$$

with the boundary conditions

$$0 \leq x \leq a, \qquad y = 0,b \qquad \frac{\partial\theta_P}{\partial y} = 0 \tag{5a}$$

$$x = 0, \qquad 0 \leq y \leq b \qquad \frac{\partial\theta_P}{\partial x} = 0 \tag{5b}$$

$$x = a, \qquad 0 \leq y \leq b \qquad \frac{\partial\theta_P}{\partial x} = \frac{1}{b} \tag{5c}$$

This Poisson solution, which also satisfies eq. (4), accounts for the total heat addition to the channel by virtue of eq. (5c) so any solutions that are added to it must not add or subtract any additional net amount of heat.

We now seek a solution of the energy eq. (4) in the form

$$\theta = \theta_P + \theta_L \tag{6}$$

If this is substituted into eq. (4) and eq. (5) is then utilized, it is found that θ_L satisfies the Laplace equation

$$\nabla^2\theta_L = 0 \tag{7}$$

The θ_L solution will be used to adjust the θ_P solution to account for the transverse conduction within the heated wall. The boundary conditions on θ are that the normal derivatives along three sides of the quadrant are zero.

$$0 \leq x \leq a, \qquad y = 0,b \qquad \frac{\partial\theta}{\partial y} = 0 \tag{6a}$$

$$x = 0, \qquad 0 \leq y \leq b \qquad \frac{\partial\theta}{\partial x} = 0 \tag{6b}$$

Along the heated long side, in the fueled region a heat balance on a wall element as shown in fig. 2 yields the equation

$$x = a,\ 0 \leq y \leq c, \quad k_f \frac{\partial T}{\partial x} = q_g + wk_w \frac{\partial^2 T}{\partial y^2}$$

With $q_g = Q/4c$, this has the equivalent form

$$\frac{\partial\theta}{\partial x} = \frac{1}{c} + w \frac{k_w}{k_f} \frac{\partial^2\theta}{\partial y^2} \tag{6c}$$

In the unheated region of the broad side, the heat balance yields

$$x = a,\ c < y \leq b, \quad \frac{\partial\theta}{\partial x} = w \frac{k_w}{k_f} \frac{\partial^2\theta}{\partial y^2} \tag{6d}$$

The boundary conditions on θ_L are found by noting that $\theta_L = \theta - \theta_P$ and hence, using eqs. (5a) to (5c) in conjunction with eqs. (6a) to (6d) give

$$0 \leq x \leq a, \qquad y = 0,b \qquad \frac{\partial \theta_L}{\partial y} = 0 \tag{7a}$$

$$x = 0, \qquad 0 \leq y \leq b \qquad \frac{\partial \theta_L}{\partial x} = 0 \tag{7b}$$

$$x = a, \qquad 0 \leq y \leq c \qquad \frac{\partial \theta_L}{\partial x} = \frac{1}{c} + w \frac{k_w}{k_f} \frac{\partial^2 \theta}{\partial y^2} - \frac{1}{b} \tag{7c}$$

$$x = a, \qquad c < y \leq b \qquad \frac{\partial \theta_L}{\partial x} = w \frac{k_w}{k_f} \frac{\partial^2 \theta}{\partial y^2} - \frac{1}{b} \tag{7d}$$

Eq. (7) with boundary conditions of eqs. (7a) to (7d) can be satisfied by a product solution of the form

$$\theta_L = \sum_{n=1,2,3,\ldots}^{\infty} A_n \cos\left(\frac{n\pi y}{b}\right) \cosh\left(\frac{n\pi x}{b}\right) \tag{8}$$

Eq. (8) immediately satisfies the conditions (7a) and (7b), and conditions (7c) and (7d) remain to be satisfied by proper evaluation of the Fourier coefficients A_n. Eq. (8) is differentiated with respect to x, equated to the boundary conditions at $x = a$, and then expanded in a Fourier series to give

$$\int_0^b A_n\left(\frac{n\pi}{b}\right) \cos^2\left(\frac{n\pi y}{b}\right) \sinh\left(\frac{n\pi a}{b}\right) dy =$$

$$\int_0^b \left(w \frac{k_w}{k_f} \left.\frac{\partial^2 \theta}{\partial y^2}\right|_{x=a} - \frac{1}{b} \right) \cos\left(\frac{n\pi y}{b}\right) dy + \int_0^c \frac{1}{c} \cos\left(\frac{n\pi y}{b}\right) dy \tag{9}$$

The integrals are carried out with the first integral on the right side being integrated twice by parts. After notation of the fact that $\left.\frac{\partial\theta}{\partial y}\right|_{\substack{x=a \\ y=b}} = 0$, this yields the expression for A_n:

$$A_n = \frac{\frac{b}{n\pi c}\sin\left(\frac{n\pi c}{b}\right) - w\frac{k_w}{k_f}\left(\frac{n\pi}{b}\right)^2\int_0^b \theta(a,y)\cos\left(\frac{n\pi y}{b}\right)dy}{\frac{n\pi}{2}\sinh\left(\frac{n\pi a}{b}\right)} \tag{10}$$

For large n, the cosh and sinh terms in eqs. (8) and (10) each become very large; hence, it is more convenient numerically to form their ratio in terms of exponential functions. This leads to the result

$$\theta_L = \sum_{n=1,2,3,\ldots}^{\infty} \bar{A}_n \cos(n\pi Y)\left[\frac{e^{-\frac{n\pi}{\Upsilon}(1-X)} + e^{-\frac{n\pi}{\Upsilon}(1+X)}}{1 - e^{-\frac{2n\pi}{\Upsilon}}}\right] \tag{11a}$$

where

$$\bar{A}_n = \frac{2}{(n\pi)^2}\frac{b}{c}\sin\left(\frac{n\pi c}{b}\right) - 2K\left(\frac{n\pi}{\Upsilon}\right)\int_0^1 \theta(1,Y)\cos(n\pi Y)\,dY \tag{11b}$$

and

$$K \equiv \frac{wk_w}{ak_f},$$

the wall conduction parameter.

The coefficient $\bar{A}_n$ contains the unknown quantity $\theta(1,Y)$ which is the dimensionless wall temperature distribution along the broad side. Out next objective is to determine the $\bar{A}_n$ in terms of known functions. Eq. (11a) is evaluated along the broad side of the channel by letting $X = 1$, and $\theta(1,Y) - \theta_p(1,Y)$ is substituted for $\theta_L(1,Y)$ on the left side to give

$$\theta(1,Y) - \theta_p(1,Y) = \sum_{n=1,2,3,\ldots}^{\infty} \bar{A}_n \cos(n\pi Y)\left(\frac{1 + e^{-2n\pi/\gamma}}{1 - e^{-2n\pi/\gamma}}\right) \tag{12}$$

$\bar{A}_n$ is then substituted from eq. (11b) to obtain

$$\theta(1,Y) - \theta_p(1,Y) = \sum_{n=1,2,3,\ldots}^{\infty} \frac{2}{(n\pi)^2}\frac{b}{c}\sin\left(n\pi\frac{c}{b}\right)\cos(n\pi Y)\left(\frac{1 + e^{-2n\pi/\gamma}}{1 - e^{-2n\pi/\gamma}}\right)$$

$$- \sum_{n=1,2,3,\ldots}^{\infty} \frac{2}{\gamma} Kn\pi \left[\int_0^1 \theta(1,\xi)\cos(n\pi\xi)\,d\xi\right]\cos(n\pi Y)\left(\frac{1 + e^{-2n\pi/\gamma}}{1 - e^{-2n\pi/\gamma}}\right) \tag{13}$$

Eq. (13) is clearly an integral equation for the broad wall temperature distribution $\theta(1,Y)$, and its solution will lead to an expression for $\bar{A}_n$ in terms of known quantities. This particular form of integral equation can be solved by applying a procedure given in ref. 9. First, we note that the integral between definite limits $\int_0^1 \theta(1,\xi)\cos n\pi\xi\,d\xi$

is a constant for each n. These constants are unknown because they involve the unknown $\theta(1,\xi)$ function. Define

$$C_n \equiv \int_0^1 \theta(1,\xi) \cos n\pi\xi \, d\xi \tag{14}$$

Eq. (13) is next multiplied by $\cos(m\pi Y)$ and integrated from $Y = 0$ to 1 to give

$$C_m - \int_0^1 \theta_p(1,Y) \cos(m\pi Y) \, dY = \frac{1}{(m\pi)^2} \frac{b}{c} \sin\left(m\pi \frac{c}{b}\right)\left(\frac{1 + e^{-2m\pi/\gamma}}{1 - e^{-2m\pi/\gamma}}\right)$$

$$- \frac{Km\pi}{\gamma} C_m \left(\frac{1 + e^{-2m\pi/\gamma}}{1 - e^{-2m\pi/\gamma}}\right) \tag{15}$$

Now define

$$E_m \equiv m\pi \int_0^1 \theta_p(1,Y) \cos(m\pi Y) \, dY \tag{16}$$

The E_m coefficients can be directly evaluated by using the θ_p from ref. 3 as given in the appendix. Eq. (16) is substituted into eq. (15) and the result solved for C_m:

$$C_m = \frac{\frac{E_m}{m\pi} + \frac{1}{(m\pi)^2} \frac{b}{c} \sin\left(m\pi \frac{c}{b}\right)\left(\frac{1 + e^{-2m\pi/\gamma}}{1 - e^{-2m\pi/\gamma}}\right)}{1 + \frac{Km\pi}{\gamma}\left(\frac{1 + e^{-2m\pi/\gamma}}{1 - e^{-2m\pi/\gamma}}\right)} \tag{17}$$

From eq. (11b), by using the definition in eq. (14), $\bar{A}_n$ can be written as

$$\bar{A}_n = \frac{2}{(n\pi)^2} \frac{b}{c} \sin\left(n\pi \frac{c}{b}\right) - 2K\left(\frac{n\pi}{\gamma}\right) C_n \tag{18}$$

The C_n from eq. (17) is substituted into eq. (18), and the result is simplified to

$$\overline{A}_n = \frac{-2KE_n + \frac{b}{c}\frac{2\gamma}{(n\pi)^2}\sin\left(\frac{n\pi c}{b}\right)}{\gamma + Kn\pi\left(\frac{1 + e^{-2n\pi/\gamma}}{1 - e^{-2n\pi/\gamma}}\right)} \tag{19}$$

By direct integration of eq. (16), with θ_P from the appendix, the E_n are found as

$$\frac{E_n}{n\pi} = -\frac{(-1)^n}{(n\pi)^2}\left(\gamma + \frac{\gamma^2}{8}G\right) + \frac{R_n}{2}\cosh\left(\frac{n\pi}{\gamma}\right)$$

$$+ \sum_{m=1,2,3,\ldots}^{\infty} S_m(-1)^m(-1)^n \frac{m\pi\gamma}{(m\pi\gamma)^2 + (n\pi)^2}\sinh(m\pi\gamma) \tag{20}$$

where G, R_n, and S_m are given in the appendix by eqs. (A2), (A5), and (A7). This completes the θ_L solution as the $\overline{A}_n$ needed to evaluate eq. (11) have now been provided in terms of known functions.

For the θ solution to be useful in practice, it must be given relative to the dimensionless fluid bulk temperature θ_b, which is defined as

$$\theta_b = \frac{1}{ab}\int_0^a\int_0^b \frac{u}{\overline{u}}\theta\,dx\,dy = \frac{1}{ab}\int_0^a\int_0^b \frac{u}{\overline{u}}\theta_P\,dx\,dy$$

$$+ \frac{1}{ab}\int_0^a\int_0^b \frac{u}{\overline{u}}\theta_L\,dx\,dy = \theta_{P,b} + \theta_{L,b} \tag{21}$$

The quantity $\theta_{P,b}$ is given in ref. 3 so only $\theta_{L,b}$ must be evaluated here. Eq. (5) is used to eliminate $u/\bar{u}$ from the definition of $\theta_{L,b}$, which gives

$$\theta_{L,b} = \int_0^a \int_0^b \theta_L \nabla^2 \theta_P \, dx \, dy \tag{22}$$

The second form of Green's theorem is used to place this in the alternative form

$$\theta_{L,b} = \oint \left(\theta_L \frac{\partial \theta_P}{\partial \nu} - \theta_P \frac{\partial \theta_L}{\partial \nu} \right) ds + \int_0^a \int_0^b \theta_P \nabla^2 \theta_L \, dA \tag{23}$$

The second integral vanishes since $\nabla^2 \theta_L = 0$. The first integral involves the normal derivatives of θ_P and θ_L on the channel boundaries. These derivatives are zero except along the heated side. Here from eq. (5c), $\partial \theta_P / \partial \nu = \partial \theta_P / \partial x = 1/b$, and hence, eq. (23) reduces to

$$\theta_{L,b} = \int_0^b \left[\theta_L(a,y) \frac{1}{b} - \theta_P(a,y) \left. \frac{\partial \theta_L}{\partial x} \right|_{x=a} \right] dy \tag{24}$$

The quantities $\theta_L(a,y)$ and $\left. \partial \theta_L / \partial x \right|_{x=a}$ are evaluated from eq. (11a) and substituted to give

$$\theta_{L,b} = \int_0^b \frac{1}{b} \sum_{n=1,2,3,\ldots}^{\infty} \overline{A}_n \cos\left(n\pi \frac{y}{b}\right)\left(\frac{1 + e^{-2n\pi a/b}}{1 - e^{-2n\pi a/b}}\right) dy$$

$$- \int_0^b \theta_P(a,y) \sum_{n=1,2,3,\ldots}^{\infty} \overline{A}_n \left(\frac{n\pi}{b}\right) \cos\left(\frac{n\pi y}{b}\right) dy \qquad (25)$$

The first integral is zero, and noting the definition of E_n in eq. (16), $\theta_{L,b}$ reduces to

$$\theta_{L,b} = - \sum_{n=1,2,3,\ldots}^{\infty} \overline{A}_n E_n \qquad (26)$$

which can be evaluated from eqs. (19) and (20).

To summarize, the solution is given as $\theta - \theta_b = (\theta_P - \theta_{P,b}) + (\theta_L - \theta_{L,b})$, where θ_P is given in the appendix, $\theta_{P,b}$ is found in ref. 3, θ_L is given by eq. (11a), where $\overline{A}_n$ is found from eq. (19), and $\theta_{L,b}$ is given by eq. (26), where E_n is found from eq. (20).

Case II. - Heating extends past the corner into the side wall. - Fig. 3 illustrates a fuel channel construction where the fuel plates extend into grooves in the side plates. Because of errors in manufacturing tolerance, the fueled region in a nuclear reactor channel might sometimes extend beyond the corner, which would tend to raise the corner temperature. The heat generation supplied by the fuel extending past $y = b$ will be treated as a source, the heat of which is conducted into

the long side at the corner. The magnitude of this heat source is $q_g e$, where, in this case, the heat generation per unit area q_g is related to the heat addition per unit channel length Q by $q_g = Q/4(b + e)$. The side plates are again assumed to be nonconductors with no internal heat generation. Equating the heat source to the peripheral heat conduction at the corner gives

$$q_g e = \frac{Qe}{4(b + e)} = wk_w \left.\frac{\partial T}{\partial y}\right|_{\substack{x=a \\ y=b}} \quad \text{or} \quad \left.\frac{\partial \theta}{\partial y}\right|_{\substack{x=a \\ y=b}} = \frac{ek_f}{(b + e)k_w w} \tag{27}$$

The solution proceeds with small modifications in the same manner as case I. The heat balance for a wall element on the long side now gives

$$k_f \left.\frac{\partial T}{\partial x}\right|_{x=a} = \frac{Q}{4(b + e)} + wk_w \left.\frac{\partial^2 T}{\partial y^2}\right|_{x=a} \tag{28}$$

Then both of the boundary conditions (7c) and (7d) on the θ_L solution are replaced by

$$x = a, \qquad 0 \leq y \leq b \qquad \frac{\partial \theta_L}{\partial x} = \frac{1}{b + e} + w \frac{k_w}{k_f} \frac{\partial^2 \theta}{\partial y^2} - \frac{1}{b} \tag{29}$$

The integral of this condition

$$\int_0^b \left.\frac{\partial \theta_L}{\partial x}\right|_{x=a} dy = \frac{b}{b + e} + w \frac{k_w}{k_f} \left.\frac{\partial \theta}{\partial y}\right|_{\substack{x=a \\ y=b}} - 1$$

By substitution of eq. (27), the integral reduces to zero, which is a necessary condition for it to be a satisfactory boundary condition for Laplace's equation.

The solution is again given by $\theta = \theta_P + \theta_L$, but the change in boundary condition makes it necessary to evaluate a new A_n. Eq. (9) is changed to

$$\int_0^b A_n\left(\frac{n\pi}{b}\right) \cos^2\left(\frac{n\pi y}{2}\right) \sinh\left(\frac{n\pi a}{b}\right) dy =$$

$$\int_0^b \left(\frac{1}{b+e} + w\,\frac{k_w}{k_f}\,\frac{\partial^2\theta}{\partial y^2}\bigg|_{x=a} - \frac{1}{b}\right) \cos\left(\frac{n\pi y}{b}\right) dy \qquad (30)$$

Carrying out the integrations and integrating the $\partial^2\theta/\partial y^2$ term twice by parts give

$$A_n\left(\frac{n\pi}{b}\right)\left(\frac{b}{2}\right) \sinh\left(\frac{n\pi a}{b}\right) = w\,\frac{k_w}{k_f}\left[(-1)^n \frac{\partial\theta}{\partial y}\bigg|_{\substack{x=a\\y=b}} - \left(\frac{n\pi}{b}\right)^2 \int_0^b \theta(a,y) \cos\left(\frac{n\pi y}{b}\right) dy\right] \qquad (31)$$

The expression for the corner derivative, eq. (27), is then substituted and the result solved for A_n:

$$A_n = \frac{(-1)^n \frac{e}{(b+e)} - w\,\frac{k_w}{k_f}\left(\frac{n\pi}{b}\right)^2 \int_0^b \theta(a,y) \cos\left(\frac{n\pi y}{b}\right) dy}{\frac{n\pi}{2} \sinh\left(\frac{n\pi a}{b}\right)} \qquad (32)$$

By comparison with eq. (10), it is seen that the only difference is the replacement of the $\frac{b}{n\pi c} \sin\frac{n\pi c}{b}$ term in the previous A_n by $(-1)^n \frac{e}{b+e}$.

The integral equation method of solution is carried out in exactly the same manner as the previous case and yields, instead of eq. (19), the $\overline{A}_n$ term

$$\overline{A}_n = \frac{-2K\mathfrak{E}_n + (-1)^n \frac{2\gamma}{n\pi}\left(\frac{\frac{e}{a}}{\gamma + \frac{e}{a}}\right)}{\gamma + Kn\pi\left(\frac{1 + e^{-2n\pi/\gamma}}{1 - e^{-2n\pi/\gamma}}\right)} \tag{33}$$

The expression for the bulk temperature $\theta_{L,b}$ remains the same for this case as eq. (26). The numerical magnitudes of $\overline{A}_n$ and $\theta_{L,b}$ will, of course, be different from those for case I.

To summarize, the solution for case II is

$$\theta - \theta_b = (\theta_P - \theta_{P,b}) + (\theta_L - \theta_{L,b})$$

where θ_P is given in the appendix, $\theta_{P,b}$ is found in ref. 3 for the case where only the broad walls are heated, and θ_L and $\theta_{L,b}$ are given by eqs. (11a) and (26), respectively, with $\overline{A}_n$ from eq. (33) and $\mathfrak{E}_n$ from eq. (20).

Limiting cases for large K or large γ. - The limiting case where $K \to \infty$ is of interest because the conducting heated wall should then become one of constant temperature. In this section only the wall temperatures will be considered. First consider the broad heated wall X = 1, Y = Y. When $K \to \infty$, the $\overline{A}_n$ from eqs. (19) and (33) become

$$\overline{A}_n(K \to \infty) = \frac{-2\mathfrak{E}_n}{n\pi}\left(\frac{1 - e^{-2n\pi/\gamma}}{1 + e^{-2n\pi/\gamma}}\right) \tag{34}$$

From eqs. (11a), (26), and (34),

$$\left[\theta(1,Y) - \theta_b\right]_{K\to\infty} = \theta_P(1,Y) - \theta_{P,b}$$

$$- \sum_{n=1,2,3,\ldots}^{\infty} \frac{2E_n}{n\pi} \cos(n\pi Y) - 2 \sum_{n=1,2,3,\ldots}^{\infty} \frac{E_n^2}{n\pi} \left(\frac{1 - e^{-2n\pi/\gamma}}{1 + e^{-2n\pi/\gamma}} \right) \tag{35}$$

Now, we expand $\theta_P(1,Y) - \theta_{P,b}$ in a Fourier cosine series

$$\theta_P(1,Y) - \theta_{P,b} = \int_0^1 \left[\theta_P(1,Y) - \theta_{P,b}\right] dY$$

$$+ 2 \sum_{n=1,2,3,\ldots}^{\infty} \cos n\pi Y \int_0^1 \left[\theta_P(1,Y) - \theta_{P,b}\right] \cos n\pi Y \, dY \tag{36}$$

But from eq. (16), the second integral is $E_n/n\pi$. Making this substitution and then substituting eq. (36) into eq. (35) to eliminate $\theta_P(1,Y) - \theta_{P,b}$ give the simplified expression

$$\left[\theta(1,Y) - \theta_b\right]_{K\to\infty} = \int_0^1 \left[\theta_P(1,Y) - \theta_{P,b}\right] dY - 2 \sum_{n=1,2,3,\ldots}^{\infty} \frac{E_n^2}{n\pi} \left(\frac{1 - e^{-2n\pi/\gamma}}{1 + e^{-2n\pi/\gamma}} \right) \tag{37}$$

Along the unheated short side a straightforward evaluation gives

$$\left[\theta(X,1) - \theta_b\right]_{K\to\infty} = \theta_p(X,1) - \theta_{P,b}$$

$$+ \sum_{n=1,2,3,\ldots}^{\infty} \bar{A}_n(K\to\infty)\left\{E_n + (-1)^n\left[\frac{e^{\frac{n\pi}{\gamma}(X-1)} + e^{-\frac{n\pi}{\gamma}(X+1)}}{1 - e^{-\frac{2n\pi}{\gamma}}}\right]\right\} \tag{38}$$

To determine the limit for finite K and $\gamma \to \infty$ requires a lengthy algebraic manipulation that is not sufficiently important to outline here. Hence, only the final result will be given:

$$\left[\theta(1,Y) - \theta_b\right]_{\gamma\to\infty} = \frac{32}{(1+K)\pi^5}(3Y^2 - 1)\sum_{m=1,3,5,\ldots}^{\infty}\frac{1}{m^5} \tag{39}$$

where

$$\sum_{m=1,3,5,\ldots}^{\infty}\frac{1}{m^5} = \frac{31}{32}(1.03693)$$

RESULTS AND DISCUSSION

The channel wall temperature distribution is a quantity of considerable interest to a designer. In figs. 4 to 7 are presented the wall temperatures as evaluated from the preceding analysis. These temperatures have been nondimensionalized by forming a ratio with $Q/4k_f$. Thus, in any figure, the magnitudes of the curves can be thought of as directly comparable in terms of temperature values when the fluid conductivity k_f and the total heat generation per unit channel length Q

are kept constant. The dimensionless wall temperatures are governed by three parameters: the wall to fluid conductivity parameter K, the channel aspect ratio γ, and either the width of the heat generating region relative to the channel width c/b, or the distance that the fuel extends past the corner e/b. The results in the figures illustrate the influence of each of the parameters.

Case I(a). - Heating extends all the way to the corner. - Fig. 4 shows the effects of varying the aspect ratio ($1 \leq \gamma \leq \infty$) and the thermal conductivity of the broad wall ($0 \leq K \leq \infty$) on the difference between the dimensionless wall and bulk temperatures when uniform heat generation takes place over the entire width (c/b = 1) of the broad walls. As the abscissa is followed from left to right, the curves extend along the wall from the center of the long side to the corner, and then from the corner to the center of the short side. As an aid to understanding the figure, consider a set of channels that have the same width of the broad sides 2b, and the same Q and k_f, but with different spacings 2a between the broad walls and different wall conductivities k_w. For a fixed K, as the aspect ratio γ increases (by a decrease in 2a), the temperatures on the heated wall and the maximum temperature, which always occurs at the corner, decrease. The reason for the temperature reductions (discussed in detail in ref. 3 for the case K = 0) is that the heat flow paths from the heated walls to the bulk of the fluid are shortened for larger γ.

The peak temperatures result from the low fluid velocities in the corner, which cause the wall temperatures to rise to compensate for the poor convection. As expected, when γ has a fixed value, an increase in K causes the wall temperatures to become considerably more uniform, and a substantial reduction in the peak temperature is obtained. This results from the increased peripheral heat conduction, which causes heat to flow from the hotter to the cooler regions of the walls and thereby reduces the imposed heat flux to the fluid at the hot spots.

To obtain a physical appreciation for the magnitudes of the K parameter, consider a channel where the thickness of the broad walls is equal to one-fourth of the spacing between them ($w/2a = 1/4$). If the walls are aluminum and the coolant is water, $K \approx 150$. For the same situation, but with walls made of stainless steel, K is reduced to 13. Finally, for a stainless-steel channel cooled by a liquid metal, K is 1 or less.

Some of the present results can be compared with those in ref. 7 (p. 385), where the Nusselt number is given for the constant-wall-temperature condition in ducts with various aspect ratios. When γ is large, the broad walls comprise most of the periphery, and when, in addition, K is large, the condition of a constant-wall-temperature duct is closely approximated. With the definitions

$$Nu = \frac{hD}{k_f}, \qquad D = \frac{4ab}{(a + b)}, \qquad \text{and} \qquad q_g = \frac{Q}{4(a + b)} = h(T_w - T_b)$$

there is obtained

$$\frac{T_w - T_b}{Q/4k_f} = \frac{4\gamma}{(1 + \gamma)^2 \, Nu} \tag{40}$$

For $\gamma = 10$, the Nusselt number from ref. 7 is 6.2 for constant wall temperature, which gives $(T_w - T_b)4k_f/Q = 0.053$ from eq. (40). Similarly for $\gamma = 20$, $Nu = 6.8$ and $(T_w - T_b)4k_f/Q = 0.027$, and for $\gamma = 100$, $Nu = 7.4$ and $(T_w - T_b)4k_f/Q = 0.0053$. These values agree quite well with the values 0.050, 0.025, and 0.0054, respectively, as computed from eq. (37) for $K \to \infty$ along the broad side of the duct ($0 \leq Y \leq 1$), as shown in fig. 4(b).

Case I(b). - Heating extends part way to the corner. - The next condition to be considered is the effect on the wall temperatures of removing the edge of the heated region a small distance (b - c) away from the corner while maintaining the total heating per unit channel length Q, a constant. The result of narrowing the heat generating region $c/b < 1$ is illustrated in fig. 5 for ducts having various aspect ratios and wall conductivities.

In figs. 5(a) and (b), which are for $\gamma = 10$ and 20, respectively, the case for $K = 1$ demonstrates the effect of c/b most clearly. The results for $K = 1$ are similar to those for zero wall conduction, $K = 0$ previously discussed in ref. 4. The most significant result for $\gamma = 10$ and 20 is the large influence exerted by small changes in c/b from unity. As c/b is decreased from unity, the corner temperature decreases sharply because of the smaller heat flux being imposed on the

region of poor convection at the corner. When c/b is decreased to about 0.96 for $\gamma = 20$ or 0.93 for $\gamma = 10$, the maximum wall temperature shifts from the vicinity of the corner to the center of the broad side. The reason for this is the formation of a heat sink by the fluid adjacent to the short side and the corner that draws heat away from the central region of the broad sides in a direction parallel to them. When $c/b \approx 0.94$ for $\gamma = 10$ and $c/b \approx 0.97$ for $\gamma = 20$ the optimum condition is achieved where the peak temperature is a minimum, and the broad wall temperatures are close to uniform. When K is increased from 1 to either 5 or 25, the wall temperatures exhibit the same general dependence on c/b as for $K = 1$, except that for higher K the wall temperatures are more uniform.

In fig. 5(c), which is for an aspect ratio of 1, the behavior is quite different from the previous results for $\gamma = 10$ and 20. As shown in fig. 4(a), when $\gamma = 1$ the temperatures along the heated wall are already quite uniform. Consequently, increasing K or removing the heat source from the corner by changing from $c/b = 1$ to 0.96 has a negligible effect on the wall-temperature distribution. Hence, for a square configuration it is not advantageous to remove the fuel loading from the corner region.

Case II. - Heating extends beyond the corner into the side wall. - Fig. 5 showed the effect of removing heat generation from the corner

region, and fig. 6 now demonstrates the opposite situation where the fuel extends beyond the corner into the side plate. Essentially this amounts to providing an additional heat source at the corner that will raise the peak temperature. The parameter e/a is the ratio formed by dividing the distance that the fuel extends past the corner by the half spacing between the plates. For a fixed value of K, an increase in e/a provides more heating at the corner thereby resulting in a higher peak temperature. As K is increased, the peak temperatures and temperature gradients in the broad wall decrease rapidly. For a K of 25, the temperature distribution is much more uniform, with the e/a parameter then having only a minor effect.

Dependence of maximum wall temperature on γ and K. - The location and magnitude of the maximum wall temperature is of great practical importance to avoid possible damage to the channel. Hence, it is of value to assess in more detail the influence of the aspect ratio and the wall conductivity parameter on the peak temperature. The maximum temperature always occurs at the corner when the heating extends all the way to the side wall $c/b = 1$ or into the side wall $e/a > 0$. To illustrate the effect of γ and K on the peak temperature, the case of $c/b = 1$ is examined in more detail as shown in fig. 7. Each curve is for a different K and gives the dependence of the maximum wall temperature on the aspect ratio. For all K values, the peak temperature decreases substantially as the aspect ratio is increased to about 10 or 20, while

beyond 20, the further decrease is small. The curves show that a lower peak temperature can result for a channel of low conductivity if the aspect ratio is kept high (e.g., $K = 1$, $\gamma = 20$) than for a channel of high K if γ is low (e.g., $K = \infty$, $\gamma = 3$). Results similar to these are indicated for situations where $c/b \neq 1$ and $e/a \neq 0$. Hence, fig. 6 provides the significant conclusion that the optimum practical aspect ratio for channels with any wall conductivity is in the range $\gamma = 10$ to 20.

There is no experimental information for laminar flow that can be used for direct comparison with the present results. There have been some experiments reported on turbulent heat transfer inside rectangular channels that had internal heat generation on all four sides. In ref. 10, a stainless-steel channel of aspect ratio 26.6 was cooled by a turbulent flow of superheated steam, and the K was approximately 300. In ref. 11, water was used to cool a stainless-steel channel of aspect ratio 20, and the K was approximately 25. In both instances there was an increase in wall temperature noted in the region adjacent to the corner; however, detailed peripheral temperature traverses were not given.

CONCLUSIONS

An analysis has been carried out to determine the temperatures in a rectangular channel with heat generating broad sides and unheated short sides under the conditions that peripheral heat conduction occurs

in the broad sides. The heat conduction within the broad walls was formulated in terms of an integral equation and coupled with the convective energy equation within the fluid. The analytical solutions for the temperatures were evaluated along the channel walls for several values of the aspect ratio, thermal conductivity of the heated wall, and width of the heat generating region on the broad side. The wall temperatures provided the following conclusions:

1. Increasing the transverse conduction in the heated broad sides produces a substantial decrease in the peak temperature and temperature gradients along the broad sides.

2. For the case where the heat generation occurs over the entire width of the broad walls, the peak temperature decreases as the aspect ratio is increased to about 20 for all values of the wall conductivity. The peak temperature then decreases only slightly as aspect ratio is further increased. This result indicates that an aspect ratio of about 20 is the optimum for minimizing the peak temperature.

3. For ducts of large aspect ratio such as 10 and 20, removing the region of heat generation a short distance away from the corner results in substantial reductions in the peak temperature. With large wall conductivity, this effect is small since the temperature distributions are already almost uniform.

4. Similarly, extending the fuel a finite distance beyond the corner can greatly increase the peak temperature unless wall conductivity is large.

ACKNOWLEDGMENT

The author would like to thank Miss Charlene Lightner, who prepared the digital computer programs for the numerical computations.

APPENDIX

SOLUTION FOR θ_P

The following is the solution for the special case of a rectangular duct with the two broad sides uniformly heated and the two short sides insulated (ref. 3):

$$\theta_P - \theta_{P,b} = \theta_\pi + \theta^* + \theta_1 + \theta_2 - \theta_{P,b} \tag{A1}$$

$$\theta_\pi = G\left\{\frac{X^4}{96} - \frac{\gamma^2 Y^2}{16} - \frac{8}{\pi^5}\sum_{n=1,3,5,\ldots}^{\infty} \frac{(-1)^{\frac{n+1}{2}}}{n^5 \cosh\left(\frac{n\pi\gamma}{2}\right)}\left[\cosh\left(\frac{n\pi\gamma}{2}\,Y\right) + \left(\frac{n\pi\gamma}{2}\right) Y \sinh\left(\frac{n\pi\gamma}{2}\,Y\right)\right]\cos\left(\frac{n\pi X}{2}\right)\right\} \tag{A2}$$

where

$$G = \left[-\frac{\gamma}{12} + \frac{16}{\pi^5}\sum_{m=1,3,5,\ldots}^{\infty}\frac{1}{m^5}\tanh\left(\frac{m\pi\gamma}{2}\right)\right]^{-1}$$

$$\theta^* = \frac{1}{2\gamma}\left(X^2 - \gamma^2 Y^2\right) \tag{A3}$$

$$\theta_1 = \sum_{n=1,2,3,\ldots}^{\infty} R_n \frac{\cosh\left(\frac{n\pi}{\gamma}\,X\right)}{\sinh\left(\frac{n\pi}{\gamma}\right)}\cos\left(n\pi Y\right) \tag{A4}$$

where

$$R_n = G\left\{\frac{4\gamma^2(-1)^n}{\pi^6 n}\sum_{m=1,3,5,\ldots}^{\infty}\frac{1}{m^3\left[\left(\frac{m\gamma}{2}\right)^2 + n^2\right]}\left[\frac{m\pi\gamma}{2} + \frac{2n^2}{\left(\frac{m\gamma}{2}\right)^2 + n^2}\tanh\left(\frac{m\pi\gamma}{2}\right)\right]\right\} \tag{A5}$$

$$\theta_2 = \sum_{n=1,2,3,\ldots}^{\infty} S_n \frac{\cosh\ (n\pi\gamma Y)}{\sinh\ (n\pi\gamma)} \cos\ (n\pi X) \tag{A6}$$

where

$$S_n = G\left\{\frac{4(-1)^n}{\pi^6 n} \sum_{m=1,3,5,\ldots}^{\infty} \frac{1}{m^3\left[n^2 - \left(\frac{m}{2}\right)^2\right]}\left[2 \tanh\ \left(\frac{m\pi\gamma}{2}\right) + \frac{m\pi\gamma}{2}\right]\right\} \tag{A7}$$

For $\theta_{P,b}$, the reader is referred to ref. 3 since the expression is too lengthy to warrant repetition herein.

REFERENCES

1. Cheng, H. M.: "Analytical Investigation of Fully Developed Laminar Flow Forced Convection Heat Transfer in Rectangular Ducts with Uniform Heat Flux." M.S. Thesis, Dept. of Mech. Eng., M.I.T., Sept. 1957.

2. Sparrow, E. M., and Siegel, R.: "A Variational Method for Fully Developed Laminar Heat Transfer in Ducts." ASME Trans., Jour. Heat Transfer, ser. C, vol. 81, no. 2, May 1959 , pp. 157-167.

3. Savino, J. M., and Siegel, R.: "Laminar Forced Convection in Rectangular Channels with Unequal Heat Addition on Adjacent Sides." Submitted to the Int. Jour. of Heat and Mass Transfer.

4. Savino, J. M., Siegel, R., and Bittner, E. C.: "Analysis of Laminar Fully Developed Heat Transfer in Thin Rectangular Channels with Fuel Loading Removed from the Corners." Preprint 125, Amer. Inst. Chem. Eng. Symposium on Nuclear Engineering Heat Transfer, Chicago (Ill.), Dec. 1962.

5. Eckert, E. R. G., and Low, G. M.: "Temperature Distribution in Internally Heated Walls of Heat Exchangers Composed of Noncircular Flow Passages." NACA Rep. 1022, 1951.

6. Baumeister, K. J., and Reilly, H. J.: "Model Study of Burnout Flux in Corners of Fuel Element Coolant Channels, Plum Brook Reactor." NASA Internal Rept. PBR-12, July 31, 1961.

7. Knudsen, J. G., and Katz, D. L.: "Fluid Dynamics and Heat Transfer." McGraw-Hill Book Co., Inc., New York, 1958.

8. Kantorovich, L. V., and Krylov, V. I.: "Approximate Methods of Higher Analysis." Interscience Publishers, Inc., New York, 1958, p. 9.

9. Hildebrand, F. B.: "Methods of Applied Mathematics." Prentice-Hall, Inc., Englewood Cliffs (N.J.), 1952, p. 406.

10. Heineman, J. B.: "An Experimental Investigation of Heat Transfer to Superheated Steam in Round and Rectangular Channels." Rept. ANL 6213, Argonne National Laboratory, Sept. 1960.

11. Levy, S., Fuller, R. A., and Niemi, R. O.: "Heat Transfer to Water in Thin Rectangular Channels." ASME Trans., Jour. of Heat Transfer, ser. C, vol. 81, no. 2, May 1959, pp. 129-143.

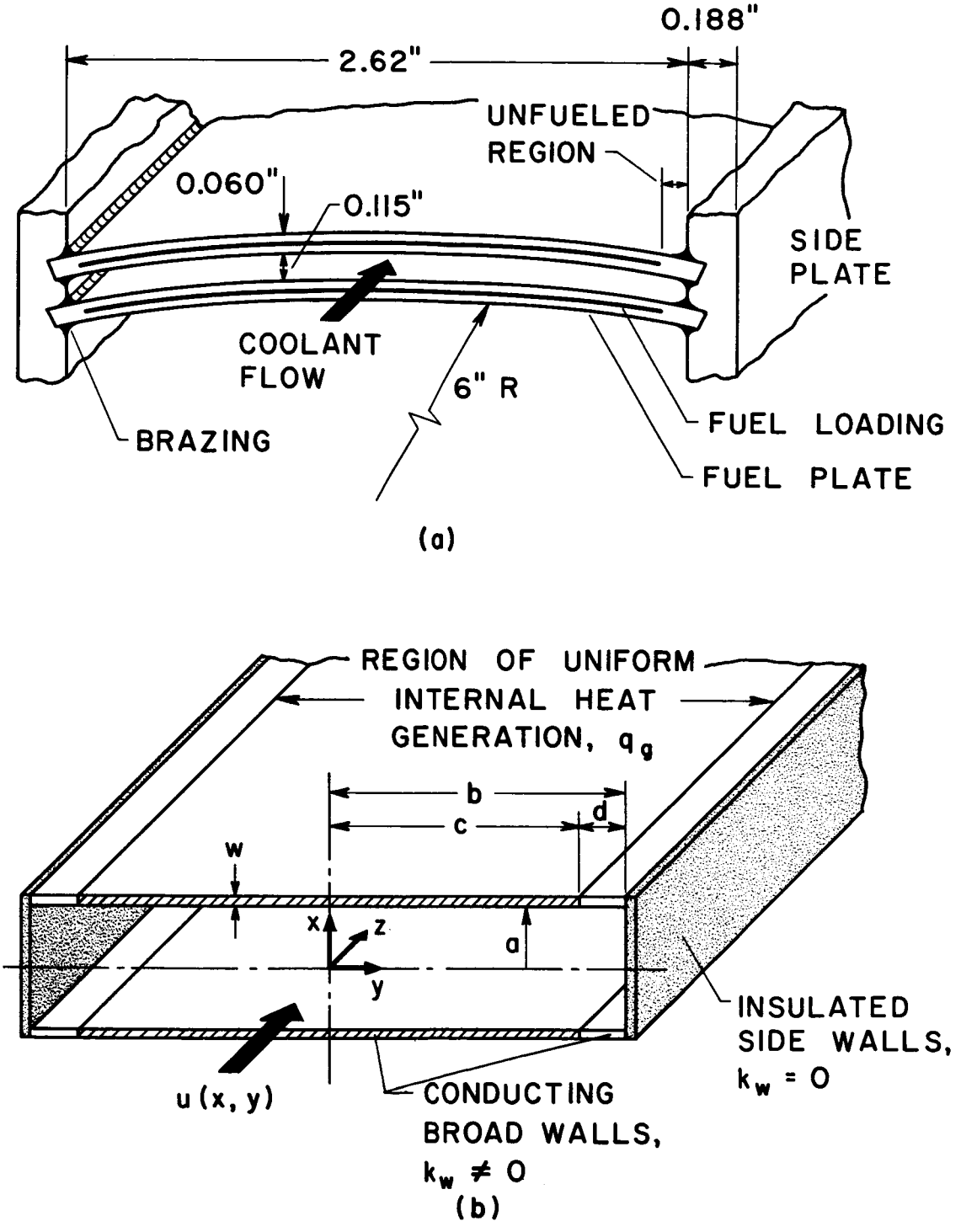

(a) Cross-section of typical cooling passage in the fuel assembly of the NASA Plum Brook reactor.
(b) Analytical model and coordinate system.

Figure 1. - Typical rectangular cooling passage inside nuclear reactor.

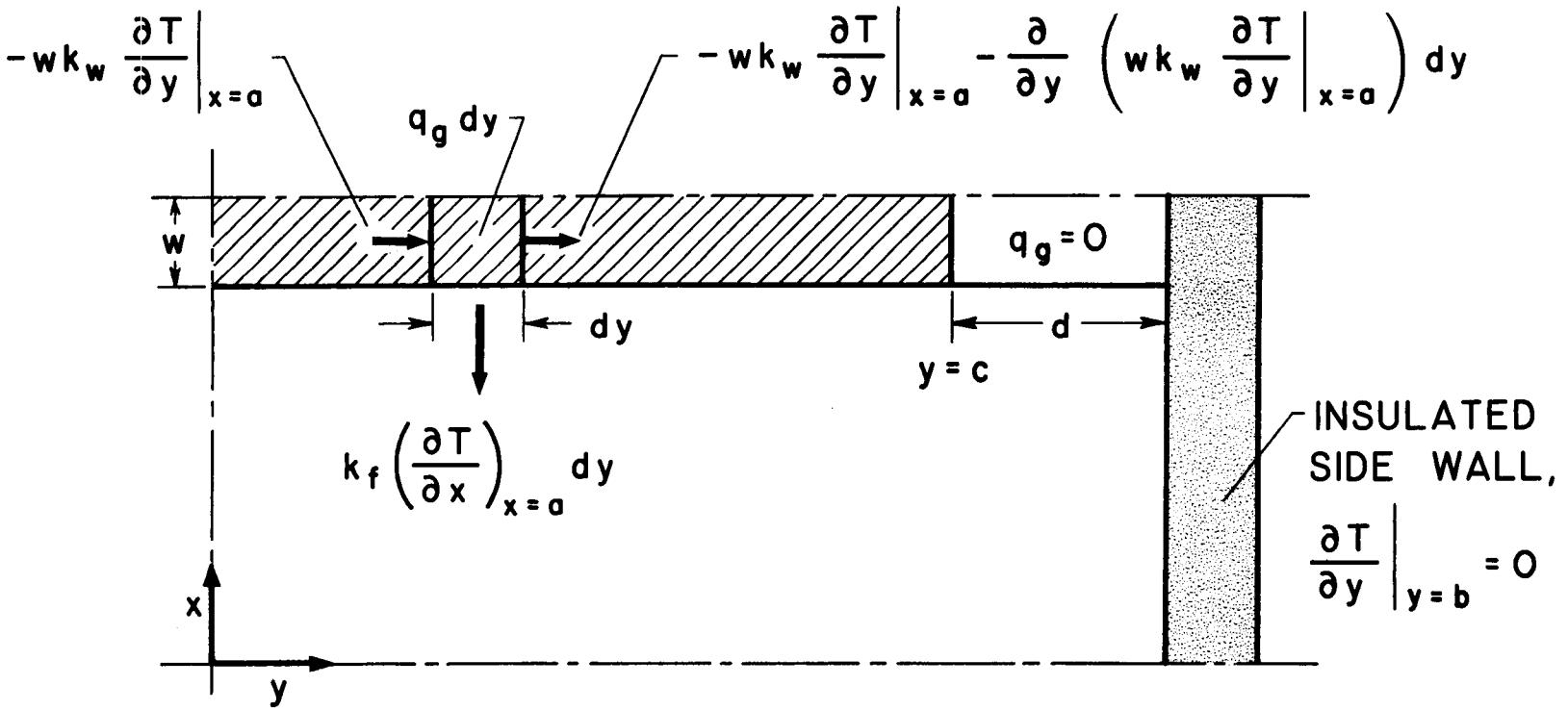

Fig. 2. - Terms for heat balance in heated region of conducting wall.

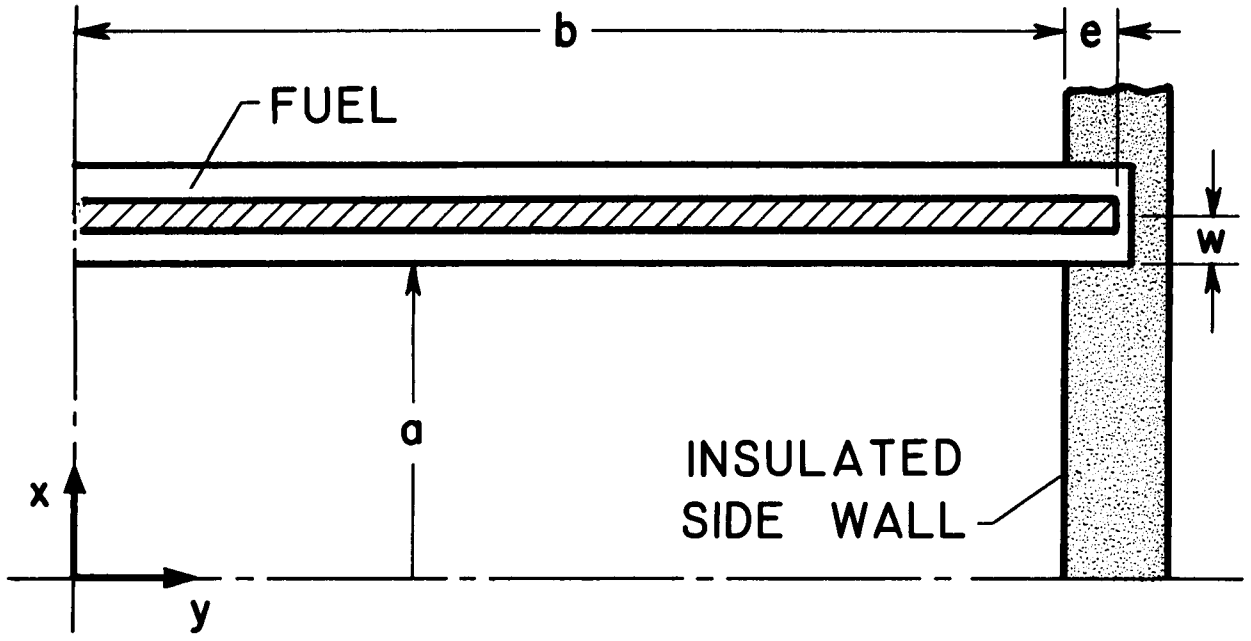

Fig. 3. - Configuration for fuel extending into side wall.

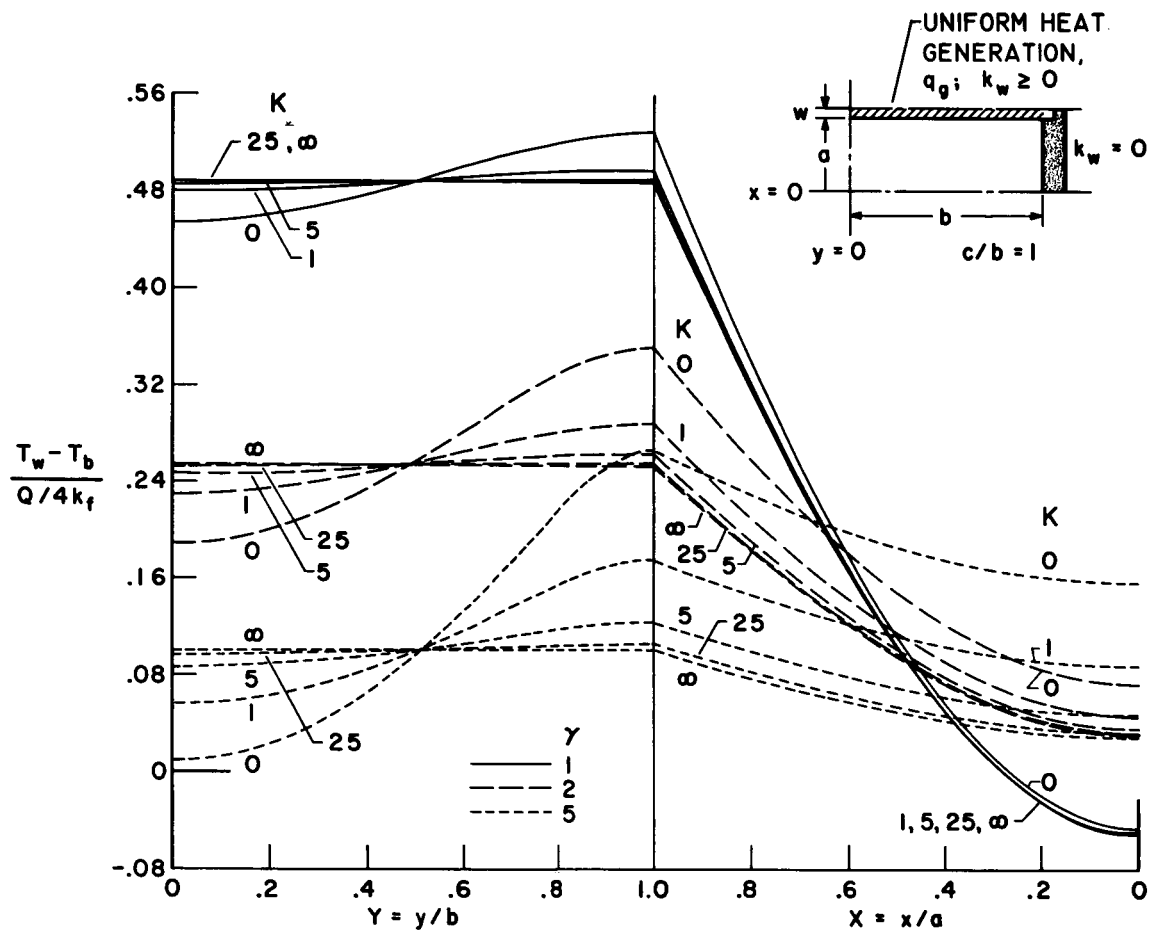

(a) Aspect ratios 1, 2, and 5.

Fig. 4. - Wall temperatures for various values of peripheral wall conduction parameter K in rectangular channels heated on entire broad sides.

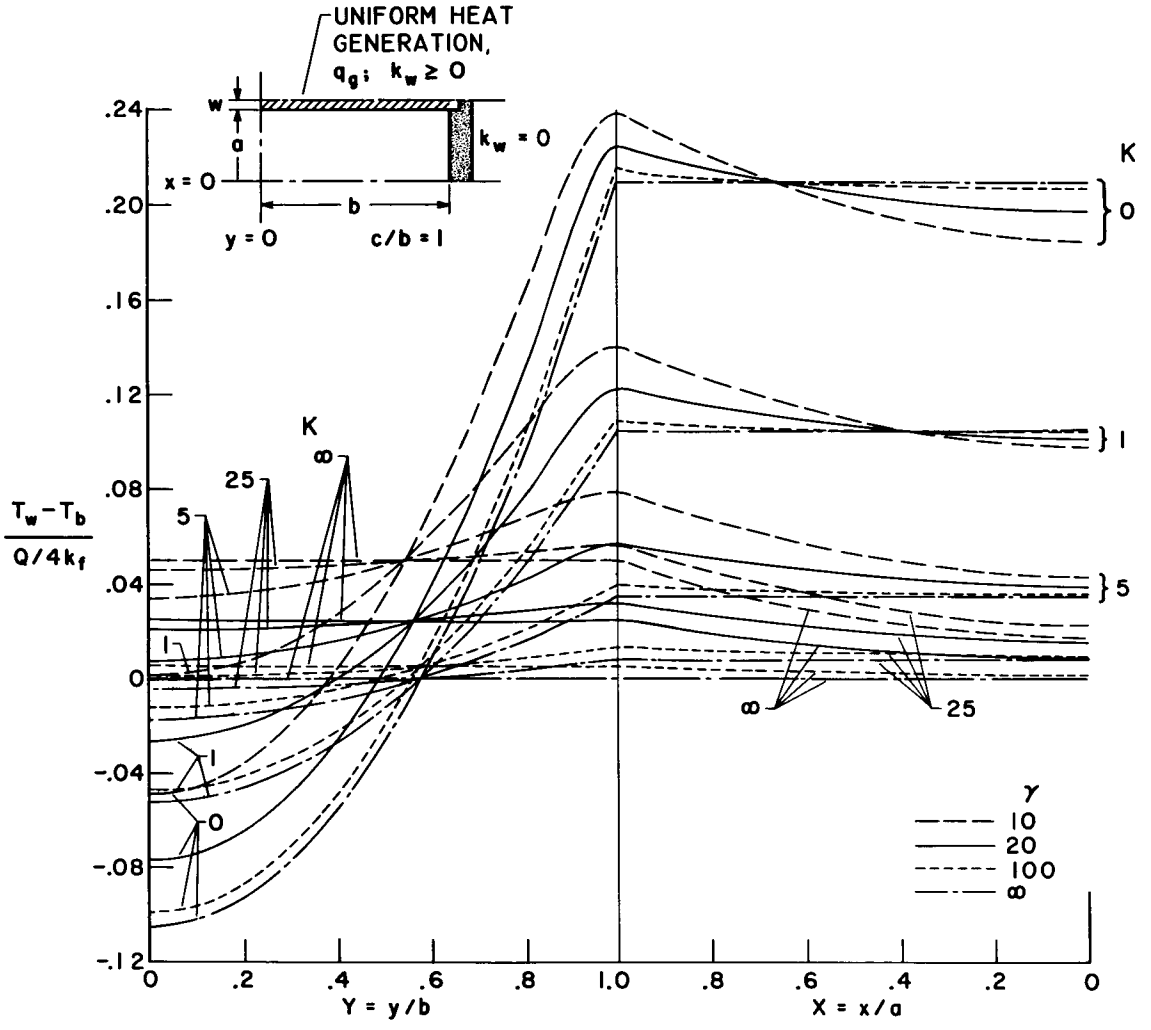

(b) Aspect ratios 10, 20, 100, and ∞.

Fig. 4. - Concluded. Wall temperatures for various values of peripheral wall conduction parameter K in rectangular channels heated on entire broad sides.

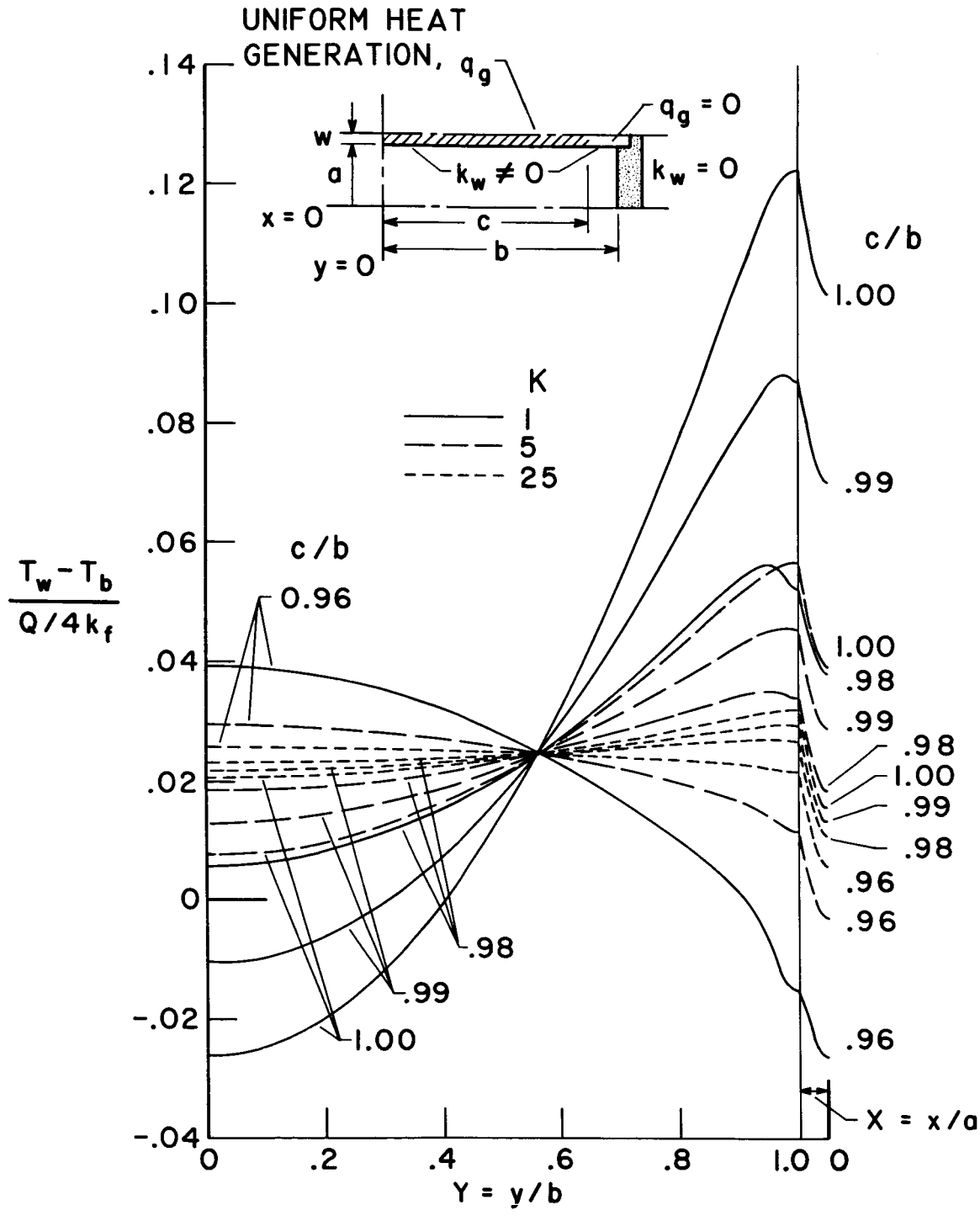

(a) Aspect ratio, $\gamma = 20$.

Fig. 5. - Effect on wall temperatures of having the heating on broad side not extend completely to the corner.

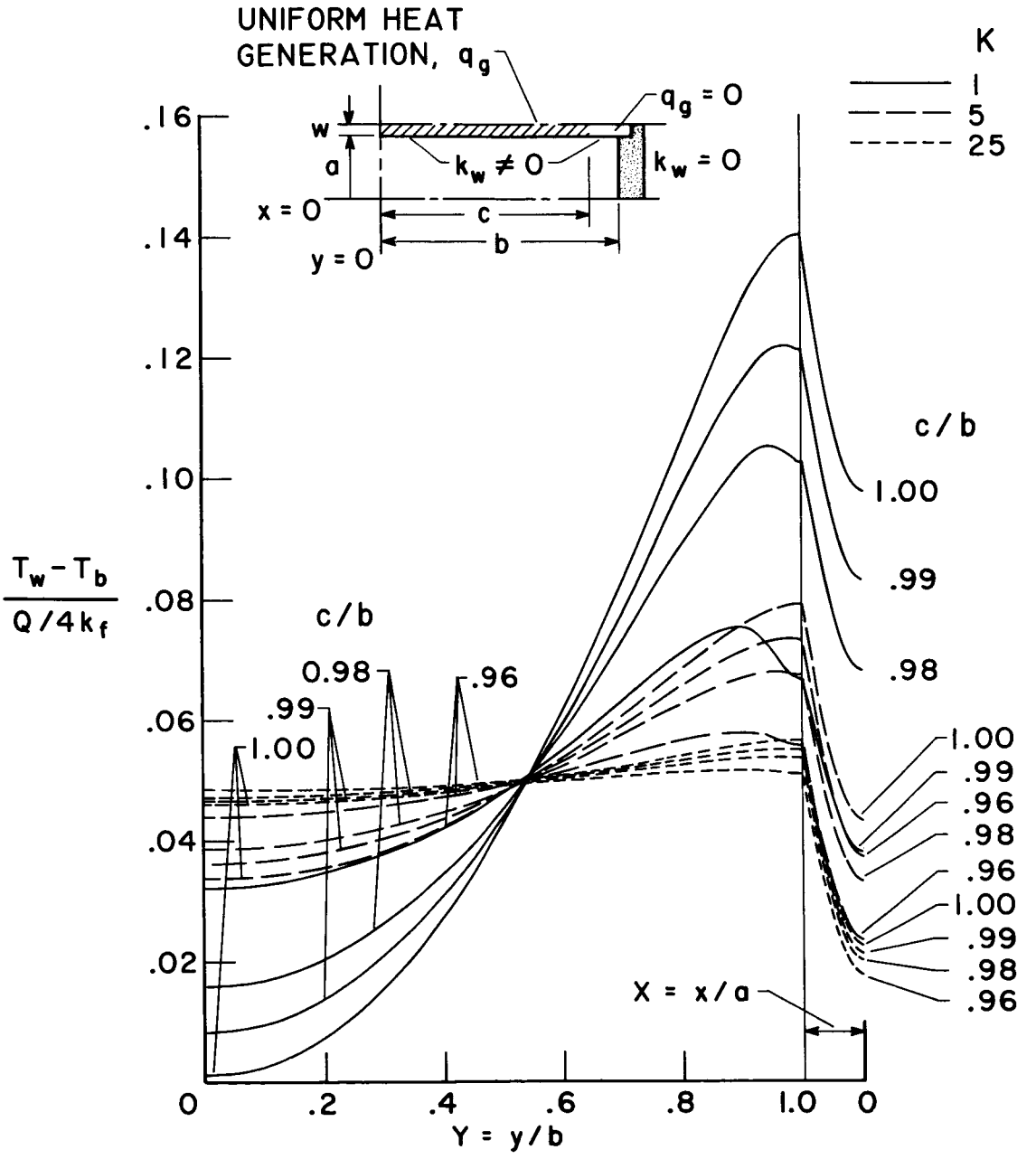

(b) Aspect ratio, $\gamma = 10$.

Fig. 5. - Continued. Effect on wall temperatures of having the heating on broad side not extend completely to the corner.

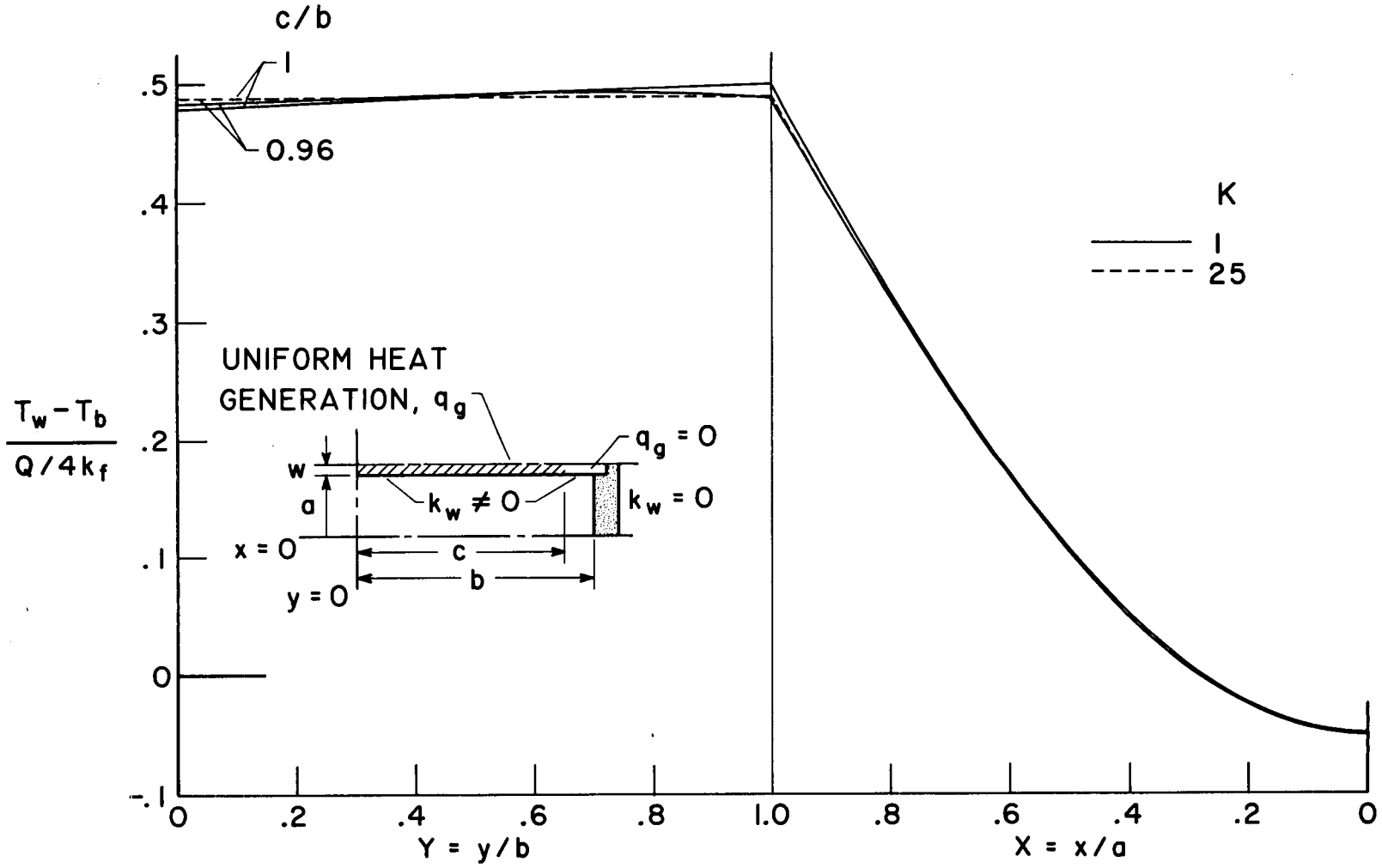

(c) Aspect ratio, $\gamma = 1$.

Fig. 5. - Concluded. Effect on wall temperatures of having the heating on the broad side not extending completely to the corner.

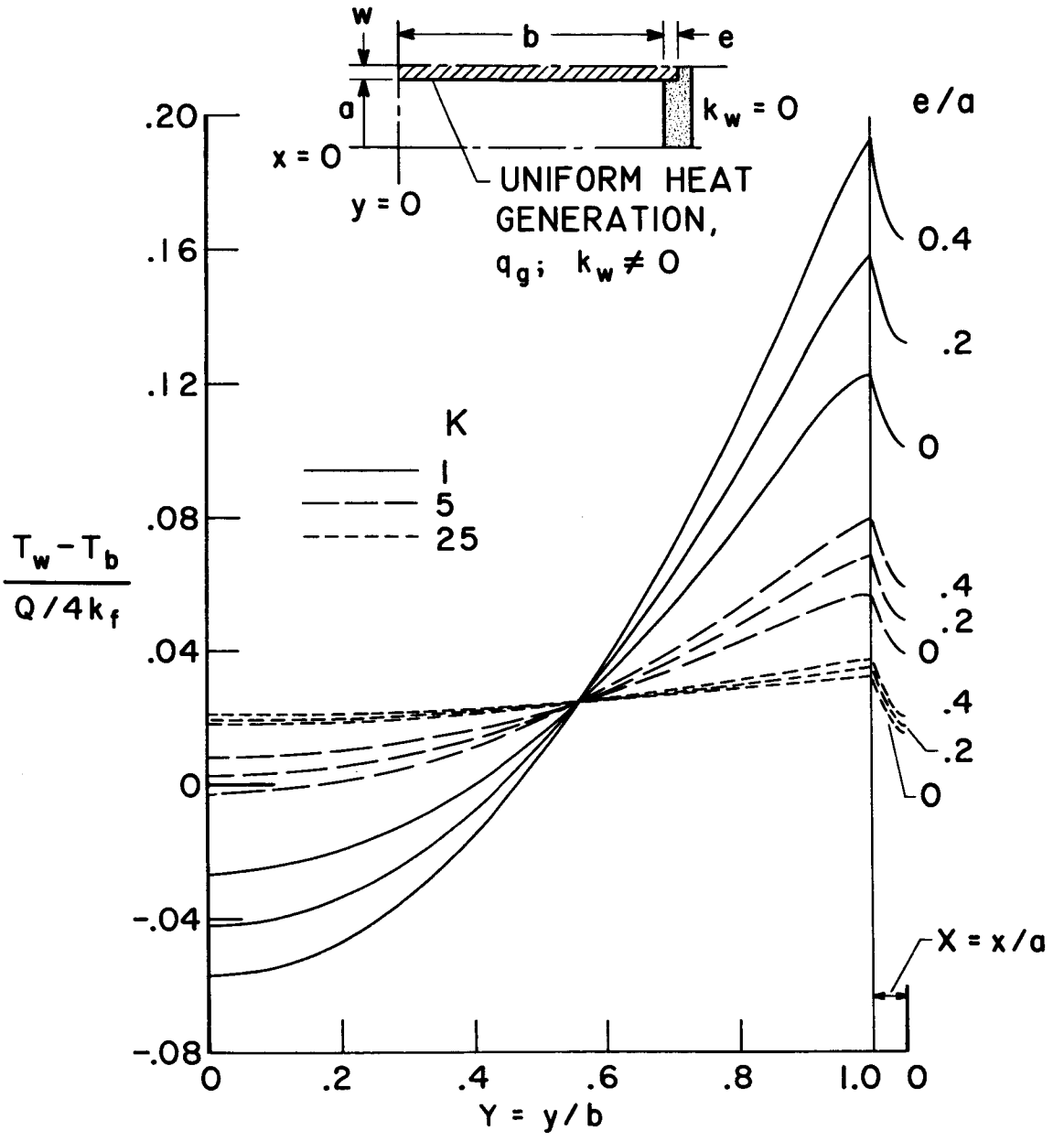

Fig. 6. - Wall temperature distributions in channel of aspect ratio 20 when heat generation extends past the corners.

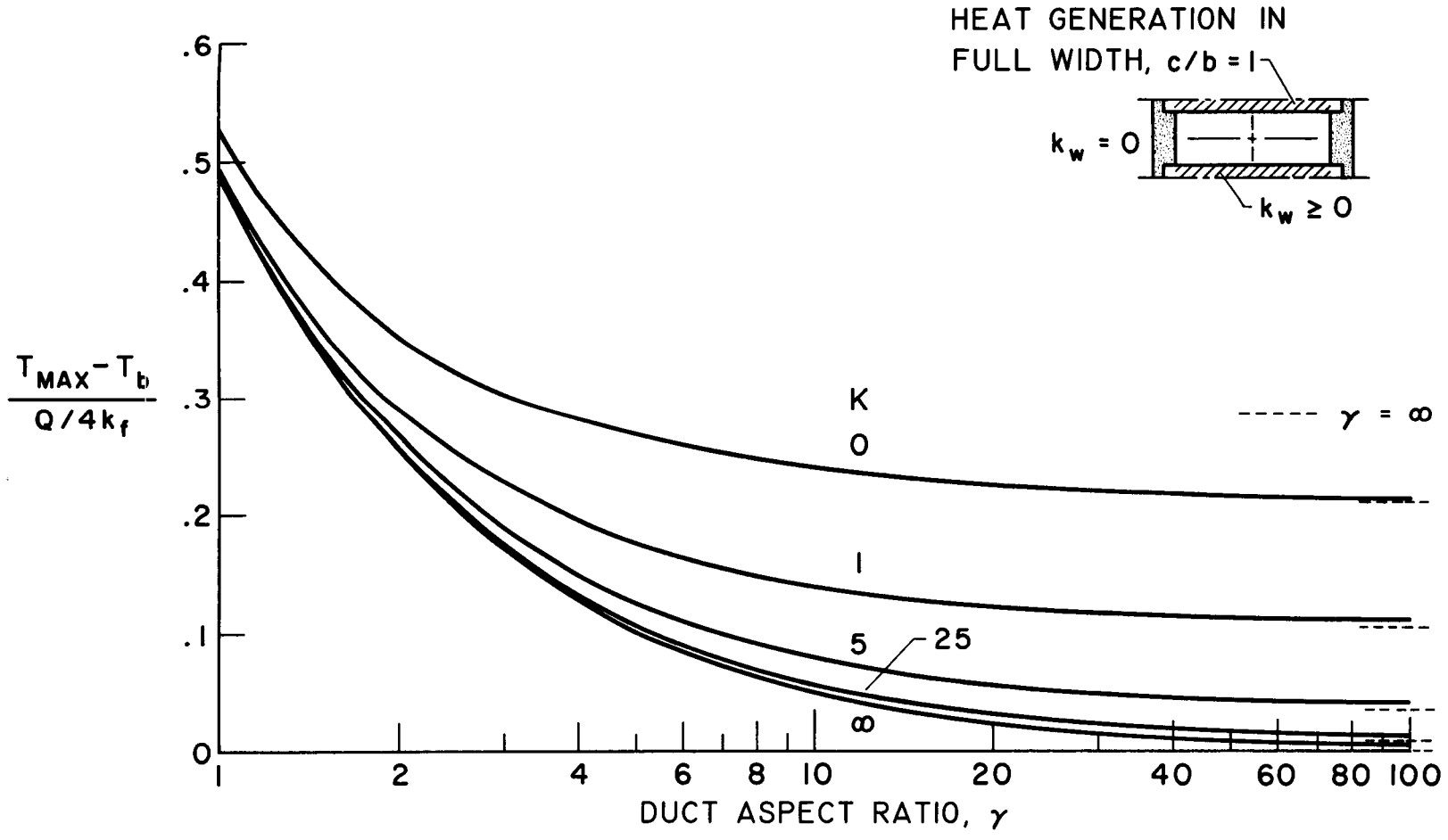

Fig. 7. - Dependence of maximum wall temperature on channel aspect ratio, γ, and wall conductivity parameter, K, with heating extending to the corner.

NASA-CLEVELAND, OHIO E-2330